SYNTHESIS, SPECTRAL, THERMAL AND QUANTUM MECHANICAL STUDIES ON 2-AMINO-4-PICOLINIUM 2-HYDROXYBENZOATE CRYSTAL

Abstract:

An organic polymorphic crystal of 2-amino-4-picolinium 2-hydroxy-benzoate (APHB) was synthesized by solvent evaporation solution growth technique at room temperature using methanol as solvent. Single crystal X-ray diffraction study revealed that the title salt belongs to monoclinic crystal system with centrosymmetric P21/c space group. The thermal characteristics of synthesized crystal were analyzed by TG-DTA study. The chemical construction has been proved by ^{1}H and ^{13}C NMR spectral techniques. The presence of various functional groups was examined by FTIR spectrum. The UV-vis-NIR spectrum was carried out to decide the optical transmittance window and lower cut-off wave length of the crystal. Theoretical calculations were performed using density functional theory (DFT) method to derive the optimized geometry, HOMO-LUMO energy gap and Mulliken charge analysis.

Keywords: Solution growth, Crystal structure, TG-DTA, Optical transmittance, DFT.

1. Introduction:

In modern years, new technologies are executed for the development of advanced materials in the realm of science research[1]. Understanding the structure in determining the properties of materials could be a significant feature of the look of materials. Physical and mechanical attributes of crystalline solids are reliant on the efficient number of atoms in a unit cell, depth and direction of packing of atoms inside the unit cell. The presence of polymorphic structures gives one of a kind opportunity for the examination of structure-property connections, since by definition the main variable among polymorphs is that of structure. For a polymorphic framework, contrasts in properties among the polymorphs must be because of contrasts in structure. In the investigation of structure-property relations for organic materials, the properties under scrutiny are because of solid collaborations between neighboring atoms, and we wish to concentrate the variations in mass properties coming about because of contrasts in the spatial connections between molecules in the crystal structure[2]. Organic molecules have been the subject of awesome consideration because of their potential applications in optical switching, frequency mixing, light emitting diodes, high speed telecommunications and other signal processing devices[3-7]. Freshly, the crystal engineering focused on common functional groups having hydrogen bond motifs in the supramolecular building blocks[8]. Several researchers studied strong interaction of carboxylic acid - pyridine synthon and reported the supramolecular crystal structures of 2-amino 4-methylpyridinium with 2-hydroxy benzoate[9], 3-hydroxybenzoate[10], 4-hydroxybenzoate[11] crystals and also reported their growth and characterization with 4-aminobenzoate[12], 4-nitrobenzoate[13], 4-nitrophenolate-4-nitrophenol[14]. These hydrogen bond donor and acceptor clusters are reciprocal and very much coordinated for pairwise holding[15-18]. Acid pyridine is energetic and famous synthons for crystal outline when they are available in various crystal structures, that is, two sensible groups at once. Aside from structural interest, amino pyridines and hydroxy benzoic acids are observed to be incredible antioxidants and initiate apoptosis which is brought about by discontinuity of DNA[19]. From the above mentioned aspects, the present work deals with the synthesis on another polymorphic supramolecular synthon of 2-amino-4-picolinium 2-hydroxybenzoate (APHB) crystals with centrosymmetric space group. The grown crystals were characterized by single crystal XRD, spectral and thermal studies. In addition, it is also aimed on theoretical calculation of optimized geometry, HOMO-LUMO energy gap and Mulliken charges of the title compound by using density functional theory (DFT).

2. Experimental Procedure:

2.1. Synthesis and growth

The crystal APHB was synthesized by taking the analar grades of 2-amino-4-methyl pyridine and 2-hydroxy benzoic acid. The calculated amounts of the reactants were separately dissolved in equimolar ratio (1:1) by using methanol solvent. The two solutions were mixed and stirred well for about 4h to complete the reaction process. After stirring, the homogeneous solution was filtered using Whatmann paper, to remove suspended impurities from the solution and then it was allowed to slow evaporation at room temperature without any disturbance. After 5 days, good quality crystals were harvested. The crystals were purified by repeated recrystallization. The reaction scheme is shown in Fig. 1.

3. Results and Discussion:

3.1. UV-Vis-NIR spectral analysis

The UV-vis-NIR spectrum of APHB crystal with a thickness of about 1 mm was recorded in the range 200 – 1100 nm using Perkin-Elmer Lambda 35 spectrophotometer at room temperature. The spectrum of APHB is shown in Fig. 2. From the spectrum, the crystal was optically transparent with a maximum transmittance of about 90%. The lower cut-off wavelength of APHB crystal was found to be 316 nm. This absorption is due to the promotion of an electron from a 'non-bonding' (lone pair) n orbital to an 'anti-bonding' π^* orbital (n $\rightarrow$ π^*).

3.2. FTIR spectral analysis

The FTIR spectrum was recorded using Bruker FTIR spectrometer by KBr pellet technique in the range of 400 – 4000 cm^{-1} and the observed spectrum of APHB is shown in Fig. 3. In the spectrum, a strong band at 3426 cm^{-1} is assigned to O – H and NH_2 asymmetric stretching vibrations. The NH_2 symmetric stretching vibration appears at 3311 cm^{-1}. The presence of aromatic C – H stretching vibration mode is observed at 3105 cm^{-1}. The absorption bands at 2971 cm^{-1} and 2667 cm^{-1} are due to CH_3 asymmetric and symmetric stretching vibrations respectively. A band appearing at 1650 cm^{-1} is due to pyridine ring stretching, C=O stretching and NH_2 scissoring vibrations[20]. The frequency observed at 1524 cm^{-1} is assigned to N – H in plane bending mode. Aromatic C=C stretching and CH_3 asymmetric scissoring vibrations are observed at 1462 cm^{-1}. The peak at 1382 cm^{-1} is due to CH_3 symmetric scissoring mode[20]. The band at 1335 cm^{-1} indicates C – N stretching vibration[14]. The C – O stretching and C=N stretching vibrations are observed at 1252 cm^{-1}. The absorption band at 1189 cm^{-1} is assigned to NH_2 rocking, O – H in-plane bending and C – CH_3 stretching vibration modes. Aromatic C – H in-plane bending[21] and CH_3 rocking mode of vibrations are identified at 1024 cm^{-1}. The NH_2 out-of plane bending vibration predicted at the frequency of 855 cm^{-1}. The C – H out-of plane bending vibrations detected at the range of 764 cm^{-1} and 660 cm^{-1}. The band at 522 cm^{-1} corresponds to in-plane bending mode of C – OH group and NH_2 wagging[20]. The spectrum shows that the absence of absorption band near 1700 cm^{-1} confirms the deprotonation of carboxyl group[19].

3.3. NMR spectral analysis

NMR spectroscopy plays a vital role in the structural confirmation of the grown crystal and the ^1H and ^{13}C NMR spectra of APHB were recorded by using DMSO solvent as shown in Figs. 4 and 5 respectively. The ^1H NMR of the title compound shows a peak at δ 2.27 corresponding to aliphatic methyl group in the picoline ring. The peak observed at δ 2.51 is due to amino and hydroxyl group protons. The protons present on 3rd and 5th positions[14] of the picoline ring produce a multiplet peak at δ 6.62. The doublet peak at δ 7.79 is due to the proton present in the 6th position of the picoline moiety. The peaks observed at δ 6.81, δ 7.32 and δ 7.86 are attributed to the protons in the benzene ring.

The ^{13}C NMR shows a peak appears at δ 21.69 confirming the presence of aliphatic methyl carbon. The peaks observed at δ 111.67 and 114.21 are due to the C3 and C5 carbons in the picoline ring. The aromatic carbons are observed at δ 116.76, δ 118.35, δ 130.83 and δ 133.60. The less intense peak[14] at δ 138.28 is due to the C6 carbon of the picoline moiety. The carbons attached with hydroxyl and amino group appears at δ 162.03. The peak at δ 174.04 corresponds to carboxylate ion carbon. Thus, the molecular structure of the compound is confirmed by ^1H and ^{13}C NMR.

3.4. Thermal studies

The TGA/DTA has been carried out using SDT Q600 V20.9 Build 20 under nitrogen atmosphere with a heating rate of 10°C/min from 25°C to 600°C. The TGA/DTA traces of APHB crystal are shown in Fig. 6. The thermal analysis reveals single stage decomposition and the compound is stable up to 152°C, which indicates that the crystal does not have any solvent in it. The decomposition pattern between 152°C and 225°C indicates complete weight loss without any residue. In the DTA curve, two major endothermic peaks are observed for the title compound. An endothermic peak at 152°C is assigned to the melting point of the crystal and the peak at 230°C corresponds to decomposition temperature of the material.

3.5. Single crystal X-ray diffraction method

Single crystal X-ray diffraction of the title salt was carried out by Bruker Kappa Apex-II diffractometer with Mo Kα radiation (λ = 0.71073 Å) at 293 K. The crystal structure solvation and refinement was performed by full-matrix least-squares method using SHELXL-97. The entire crystallographic data and refinement parameters are presented in Table 1. The APHB crystallizes in the monoclinic system with centrosymmetric space group P21/c. The ORTEP view of the grown crystal with 50% probability is shown in Fig. 7. In the ORTEP view, the two asymmetric units of APHB crystal consists of 2-amino-4-picolinium cation ($C_6H_7N_2^+$) and 2-hydroxy benzoate anion ($C_7H_5O_3^-$). It was attained by the proton transfer from carboxylic group of 2-hydroxy benzoic acid to ring nitrogen (N1) of picoline. In the title salt, the 2-amino group (N2) and protonated nitrogen atom (N1) of the cation are hydrogen bonded to carboxylate oxygen atoms (O2 and O3) of the anion through a pair of N–H…O hydrogen bonds. This proton transformation is confirmed by the bond length of N1–H1a (0.86 Å), which is shorter than the neutral N–H bond length (0.938 Å) and also carboxylate anion C7–O2 (1.269 Å), C7–O3   (1.254 Å) almost have the same bond length due to the presence of resonance, which is longer than the normal C=O bond length (1.22 Å). The bond angle of the protonated N1 atom has increased in C1–N1–C5 (121.61 (15)º), higher than the bond angle of 117.3 (1)º in neutral 2-amino-4-picoline. The angle of O3–C7–O2 (122.75 (16)º) is deviated from the normal bond angle of 120º. The two intra molecular hydrogen bonding interactions are also observed in O1–H1B…O2 and O4 – H4C…O5 forming S(6) ring. Hemamalini *et al.* reported the same crystal structure having two asymmetric moieties at 100 K, showing that one of the asymmetric moieties has aromatic π – π stacking interactions between the cations and anions, whereas the other moiety is to be planar. But in the present study, both the asymmetric moieties are stacked with each other and are designated as the 'sandwich-herringbone structure'[22] due to the presence of edge to face aromatic π – π stacking interactions between the cations and anions. A weak trifurcated hydrogen bonding interactions (C18 – H18…O1) arise from pyridinum C – H with the hydroxyl group. In addition to these, normally 2-amino substituted pyridine moieties upon protonation leads to the formation of hydrogen bonded ring motif (R2, 2(8)) in its crystal structure[23]. In the title crystal also, a pair of N – H…O hydrogen bond leads to the formation of R2, 2(8) motifs with eight membered ring between the each cation and anion and it is viewed in the packing of the crystal along 'b' axis (Fig. 8). The hydrogen bonding interactions are illustrated in Table 2.

3.6. Optimized geometry

The optimized molecular structure of APHB is shown in Fig. 9. The geometrical parameters attained from the DFT method compared with pertinent experimental data are tabulated in Table 3 and 4. It shows that the slight variations between the molecular geometry in vapour phase (calculated) and in solid phase (experimental) due to extended hydrogen bonding and stacking interactions between the calculated and experimental geometric parameters[24].   The larger bond lengths of C1–C7 (1.493 Å), C1–C6 (1.417 Å), C17–C18 (1.420 Å), C18–C22 (1.506 Å) and C19–C20 (1.421 Å) is due to the substitution in the ring. The calculated bond lengths of C7–O8 and C7–O9 are found to be 1.301 Å and 1.251 Å respectively. The shortening of C7–O8 bond from the normal C–O bond shows double bond nature due to resonance in the carboxyl group. The geometrical parameters of O8–H11 (1.658 Å), O8–H24 (1.658 Å) and O9–H31 (1.658 Å) are in good agreement within hydrogen bonding limit. These distances are considerably shorter than the van der waals radii (2.75 Å) between O and H atoms due to the hydrogen bridge which tends to push the two hetero atoms closer to each other. This indicates the existence of O–H…O and N–H…O hydrogen bonding network[25]. The presence of N–H…O hydrogen bonding shorten the bond lengths of C16–N21 (1.353 Å), C20–N21 (1.360 Å),   C20–N23 (1.335 Å). The bond angles of N21–H24…O8 (178.8°) and N23–H31…O9 (175.3°) are nearly to be 180°, which shows a strong intermolecular hydrogen bonding in the molecule.

3.7. Frontier molecular orbital analysis

The frontier molecular orbitals can offer a reasonable prediction of the excitation properties and characterizes the molecular chemical reactivity, kinetic stability and chemical hardness of the molecule[26]. The electronic transition energy in the system can be calculated by the difference between the highest occupied molecular orbital (HOMO) and the lowest unoccupied molecular orbital (LUMO). The HOMO is the outermost orbital that acts as an electron donor whereas LUMO is the innermost orbital that acts as electron acceptor[14]. The positive and negative phases are represented in red and green colour respectively. The HOMO-LUMO energies and the energy gap for APHB molecules have been calculated using B3LYP level with 6-31G(d,p) basis set. The 3D plots of the HOMO-LUMO for the APHB is shown in   Fig. 10. From the figure, the HOMO is localized on the 2-hydroxybenzoate anion and the LUMO is localized mainly on all the atoms of 2-amino-4-picolinium cation.

The energy gap between HOMO (-5.2801 eV) to LUMO (-1.5725 eV) of the molecule is found to be 3.707 eV. The calculated energy gap of HOMO-LUMO indicates the electron density transfer through hydrogen bond within the molecule.

3.9. Mulliken charge analysis

The atomic charge distribution in APHB was calculated by Mulliken population analysis[27]. The charge distribution of APHB (Fig. 11) shows the carbon atoms C2, C3, C4, C5, C17, C19 and C22 possess negative charges, whereas the other carbon atoms C1, C6, C7, C16, C18 and C20 are positively charged. Compared to other positive charge carbon atoms, the C7 (0.613 e) and C20 (0.587 e) carbon atoms have large positive charge, since these carbon atoms are attached to electronegative atoms O and N. The oxygen atoms O8 (-0.691 e), O9 (-0.588 e), O10 (-0.584 e) and nitrogen atoms N21 (-0.615 e), N23 (-0.674 e) have more negative charges indicating the intra (O–H…O) and inter (N–H…O) molecular hydrogen bonding network. In this charge analysis all the hydrogen atoms are positively charged. The highest values of charge are noticed for H11, H24 and H31 which are involved in hydrogen bonding. The charge increase at the hydrogen atoms taking part in hydrogen bonding is also a clear manifestation of hydrogen bonding.

Conclusions:

Single crystals of APHB were grown by slow evaporation method using methanol solvent. The UV spectrum showed a good optical transmittance in the visible region and the lower cut-off wave length at 316 nm. The FTIR and NMR spectra revealed the presence of the functional groups and the molecular structure. The thermal stability and decomposition stage of the compound were confirmed by TGA/DTA analysis. The crystal belongs to monoclinic system with centrosymmetric space group P21/c as confirmed by the single crystal X-ray diffraction study. Based on the density functional theory, optimizations carried out at B3LYP level with 6-31G(d,p) basis set for APHB indicated that the subsistence of strong O–H…O and N–H…O hydrogen bonding interactions. The HOMO-LUMO energy gap analysis supports the electron density within the molecule. The Mulliken charge analysis explains the possibilities of hydrogen bonding.
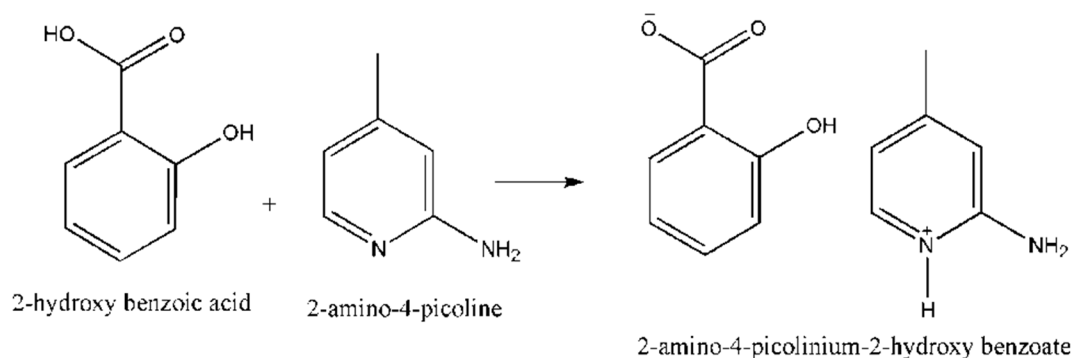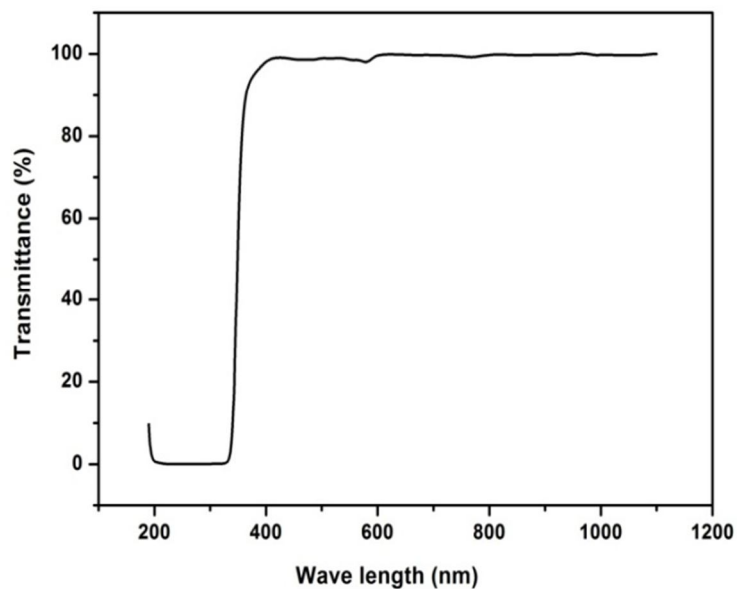

Fig. 1. Reaction scheme of APHB
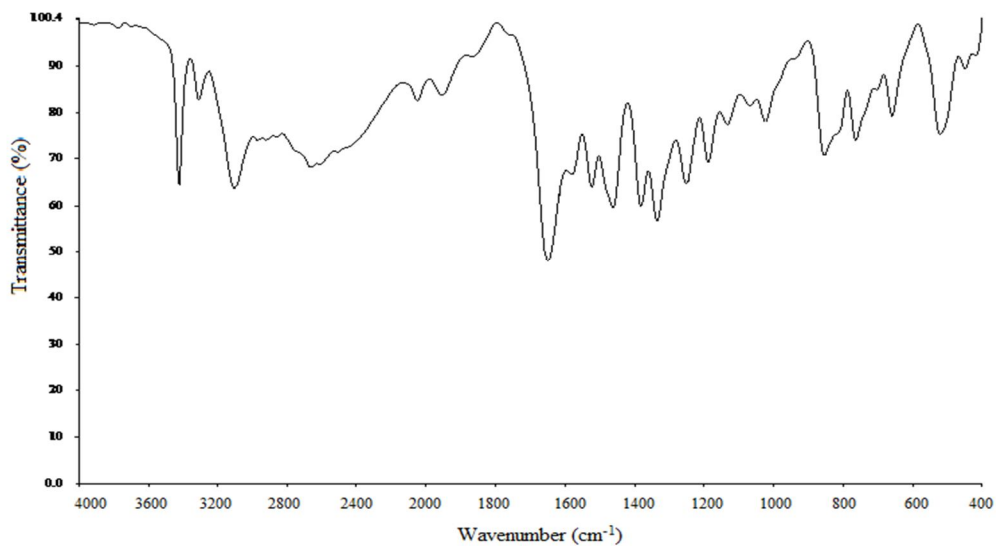
Fig. 2. UV-Vis-NIR transmittance spectrum of APHB
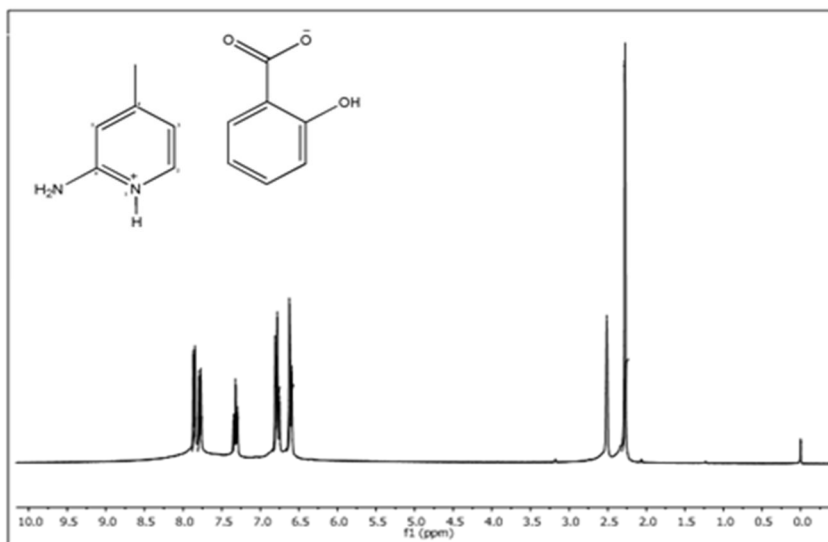

Fig. 3. FTIR spectrum of APHB
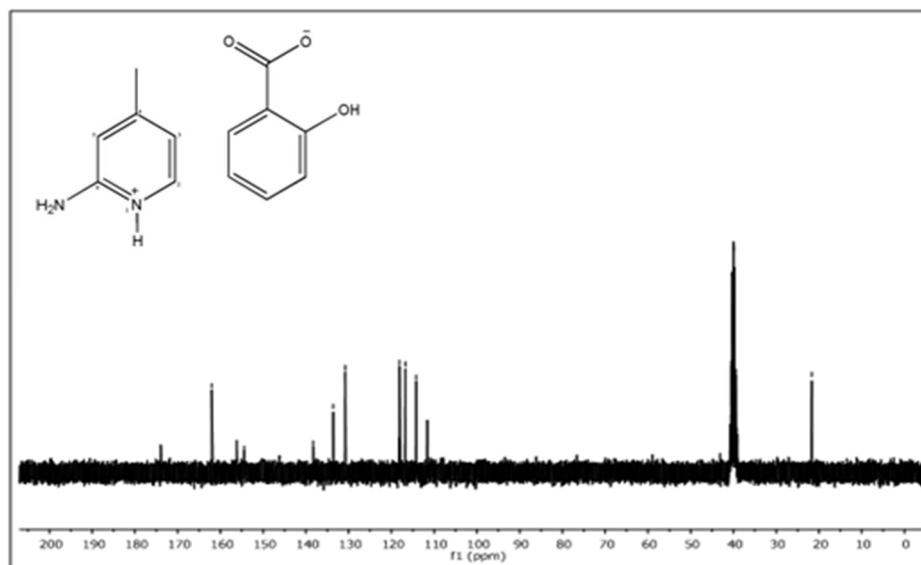
Fig. 4. ^{1}H NMR spectrum of APHB

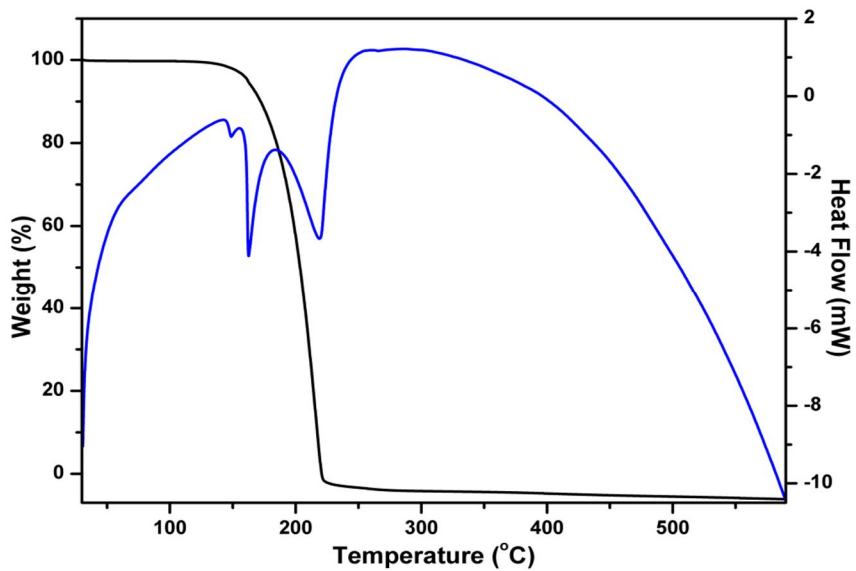**Fig. 5.** ^{13}C NMR spectrum of APHB

Fig. 6. TGA/DTA curve of APHB
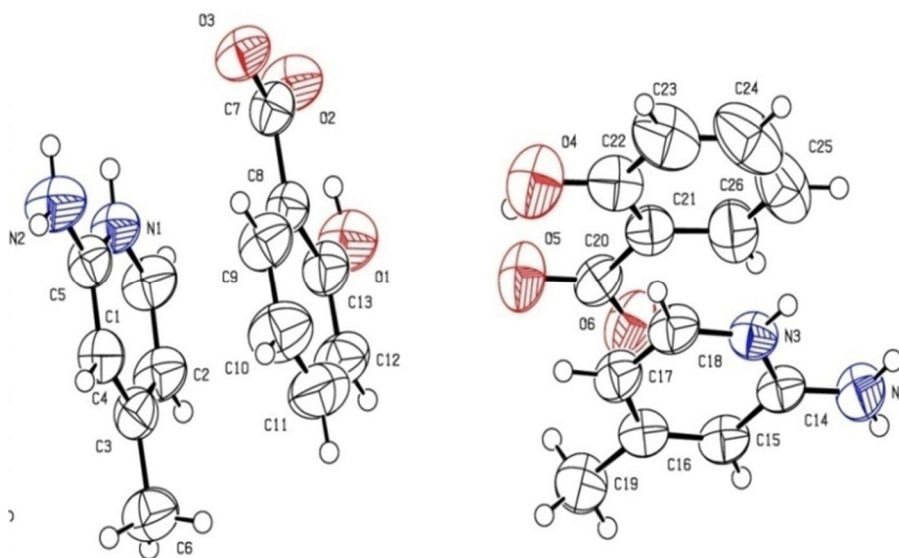

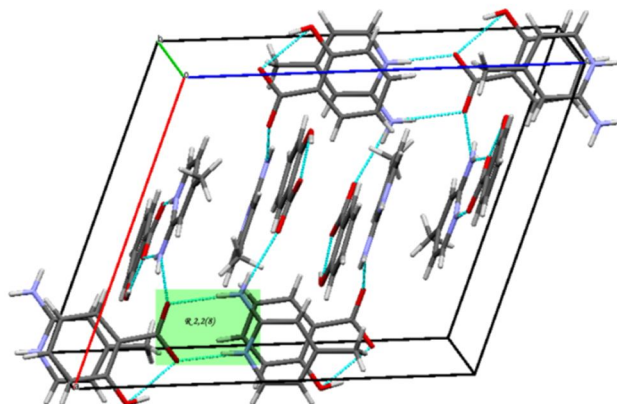**Fig. 7.** ORTEP view of APHB

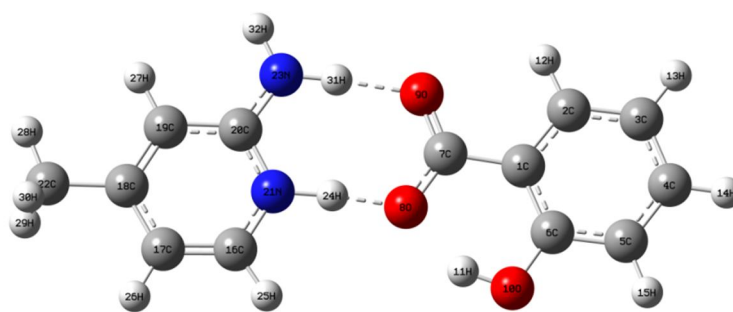**Fig. 8.** Crystal packing arrangement along b-axis

Fig. 9. Optimized structure of APHB

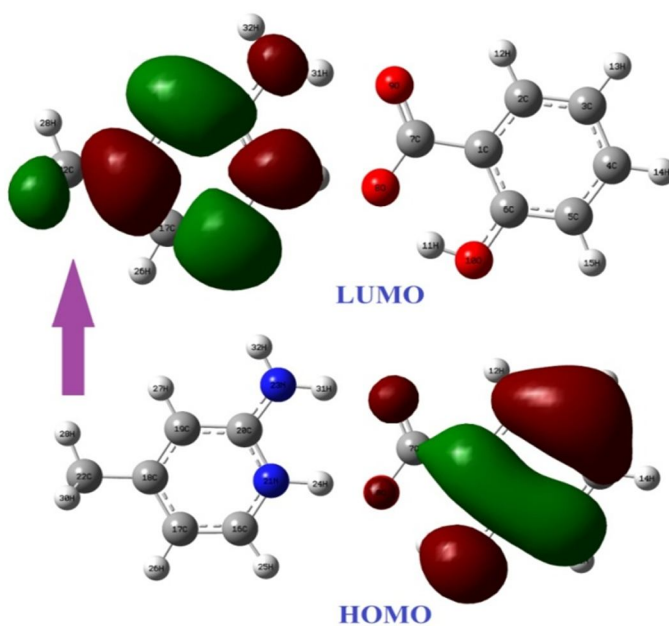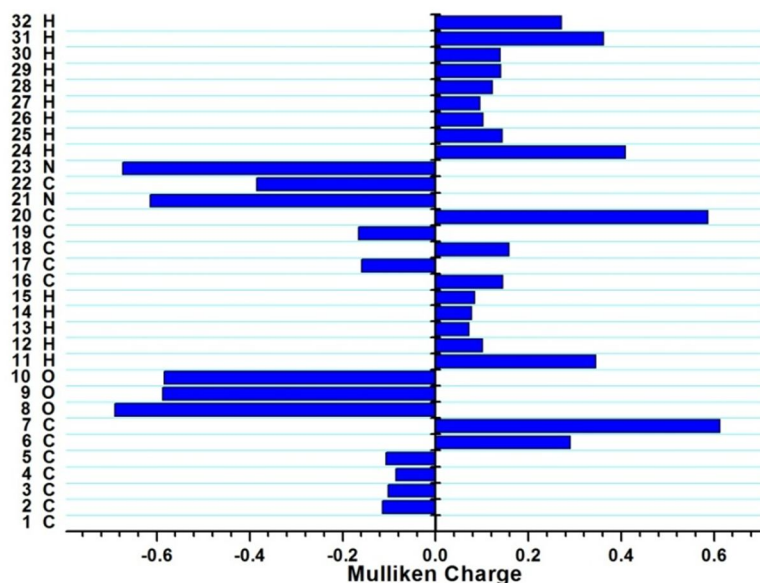**Fig. 10.** HOMO-LUMO energy gap of APHB

Fig. 11. Mulliken charge distribution of APHB

Table 1 Crystal data and structure refinement of APHB

Empirical formula	$C_{26}H_{28}N_4O_6$
Formula weight	492.52
Crystal system	Monoclinic
Space group	P21/c
Unit cell dimensions	a = 12.668 (5) Å
	b = 13.804 (5) Å
	c = 15.400 (5) Å
	$\alpha = \gamma = 90\ (5)°,\ \beta = 111.235\ (5)°$
Volume (V)	2510.1 (16) Å^3
Temperature	293 K
Z, Calculated density	4, 1.303 Mg m^{-3}
Radiation	Mo $K\alpha$ 0.71073 Å
F(000)	1040
Absorption coefficient (μ)	0.09 mm^{-1}
Crystal size	$0.20 \times 0.15 \times 0.10$ mm
θ range	1.7° - 28.4°
Index ranges	$-16 \leq h \leq 16$
	$-18 \leq k \leq 17$
	$-20 \leq l \leq 20$
Reflections collected/independent	24328/6273
R_{int}	0.033
Reflections with I > 2σ(I)	3743
Goodness-of-fit (GOF) on F^2	1.03
R indices (all data)	$R_1 = 0.049$, $wR_2 = 0.151$
Extinction coefficient	0.0117 (12)
Largest difference peak and hole	0.30 and -0.24 e Å^{-3}

Table 2 Hydrogen bonding interactions of APHB

D–H…A	d(D–H)	d(H…A)	d(D…A)	<D–H…A	Symmetry
N(1)–H(1A)…O(3)	0.86	1.89	2.746 (2)	172	3 – x, 1 – y, 2 – z
O(1)–H(1B)…O(2)	0.82	1.78	2.509 (2)	147	-
N(2)–H(2A)…O(2)	0.86	1.97	2.821 (2)	173	3 – x, 1 – y, 2 – z
N(2)–H(2B)…O(6)	0.86	2.07	2.887 (2)	158	1+x, 1/2 – y, 1/2+z
N(3)–H(3)…O(5)	0.86	1.80	2.651 (2)	173	x, 1/2 – y, -1/2+z
N(4)–H(4A)…O(6)	0.86	2.01	2.861 (2)	172	x, 1/2 – y, -1/2+z
N(4)–H(4B)…O(3)	0.86	2.04	2.892 (2)	171	x, 1/2 – y, -1/2+z
O(4)–H(4C)…O(5)	0.82	1.82	2.542 (2)	146	-
C(18)–H(18)…O(1)	0.93	2.51	3.382 (3)	156	x, 1/2 – y, -1/2+z

Table 3 Optimized geometrical bond distance of APHB on B3LYP/6-31G(d,p) basis set

Bond length	Value (Å)		Bond length	Value (Å)	
	Cal.	Expt.		Cal.	Expt.
C1–C2	1.371	1.343 (3)	C7–C8	1.493	1.488 (2)
C1–N1	1.353	1.351 (2)	C8–C9	1.404	1.378 (2)
C1–H1	1.085	0.9300	C8–C13	1.417	1.404 (2)
C2–C3	1.420	1.404 (2)	C9–C10	1.388	1.369 (3)
C2–H2	1.084	0.9300	C9–H9	1.085	0.9300
C3–C4	1.380	1.365 (2)	C10–C11	1.402	1.375 (3)
C3–C6	1.506	1.491 (3)	C10–H10	1.086	0.9300
C4–C5	1.421	1.396 (2)	C11–C12	1.388	1.360 (3)
C4–H4	1.085	0.9300	C11–H11	1.087	0.9300
C5–N2	1.335	1.327 (2)	C12–C13	1.405	1.390 (3)
C5–N1	1.360	1.340 (2)	C12–H12	1.085	0.9300
C6–H6A	1.092	0.9600	C13–O1	1.347	1.347 (2)
C6–H6B	1.095	0.9600	N2–H2A	1.054	0.8600
C6–H6C	1.095	0.9600	N2–H2B	1.007	0.8600
C7–O3	1.251	1.254 (19)	N1–H1A	1.130	0.8600
C7–O2	1.301	1.269 (2)	O1–H1B	0.992	0.8200

Table 4 Optimized geometrical bond angle of APHB on B3LYP/6-31G(d,p) basis set

Bond angle	Value (°)		Bond angle	Value (°)	
	Cal.	Expt.		Cal.	Expt.
C2–C1–N1	122.1	121.47 (16)	C9–C8–C7	119.2	120.99 (14)
C2–C1–H1	122.9	119.3	C13–C8–C7	121.8	120.73 (15)
N1–C1–H1	115.0	119.3	C10–C9–C8	121.4	121.53 (18)
C1–C2–C3	118.6	119.24 (15)	C10–C9–H9	121.3	119.2
C1–C2–H2	120.3	120.4	C8–C9–H9	117.3	119.2
C3–C2–H2	121.1	120.4	C9–C10–C11	119.1	119.7 (2)
C4–C3–C2	118.7	118.28 (16)	C9–C10–H10	120.4	120.1
C4–C3–C6	121.3	121.77 (16)	C11–C10–H10	120.4	120.1
C2–C3–C6	120.0	119.93 (15)	C12–C11–C10	120.7	120.5 (2)
C3–C4–C5	120.8	121.28 (15)	C12–C11–H11	119.3	119.8
C3–C4–H4	120.7	119.4	C10–C11–H11	119.9	119.8

C5–C4–H4	118.4	119.4	C11–C12–C13	120.3	120.38 (19)
N2–C5–N1	117.8	118.61 (16)	C11–C12–H12	121.6	119.8
N2–C5–C4	124.0	123.30 (15)	C13–C12–H12	118.1	119.8
N1–C5–C4	118.2	118.09 (14)	O1–C13–C12	118.0	118.80 (16)
C3–C6–H6A	111.8	109.5	O1–C13–C8	122.6	121.60 (17)
C3–C6–H6B	110.6	109.5	C12–C13–C8	119.4	119.60 (18)
C3–C6–H6C	110.6	109.5	C5–N1–C1	121.4	121.61 (15)
H6A–C6–H6B	108.3	109.5	C5–N1–H1A	120.2	119.2
H6A–C6–H6C	108.3	109.5	C1–N1–H1A	118.3	119.2
H6B–C6–H6C	108.3	109.5	C5–N2–H2A	120.8	120.0
O3–C7–O2	123.6	122.75 (16)	C5–N2–H2B	118.9	120.0
O3–C7–C8	119.9	119.96 (14)	H2A–N2–H2B	0	120.0
O2–C7–C8	116.5	117.28 (14)	C13–O1–H1B	105.2	109.5
C9–C8–C13	119.0	118.27 (17)			

References:

1. Eaton DF, Nonlinear optical materials. Science 1991; 253: 281-287.
2. Bernstein J, Crystal growth, polymorphism and structure-property relationshipsin organic crystals. J Phys D: Appl Phys 1993; 26: B66-B76.
3. Chen T, Sun Z, Li L, Wang S, Wang Y, Luo J, et al. Growth and characterization of a nonlinear optical crystal. 2, 6-diaminopyridinium 4-nitrophenolate 4-nitrophenol. J Cryst Growth 2012; 338: 157-161.
4. Breitzar JG, Diott DD, Iwaki LK, Kirkpatrick SM, Rauchturs TB, Third-Order Nonlinear Optical Properties of Sulfur-Rich Compounds. J Phys Chem A 1999; 103: 6930-6937.
5. Datta A, Pati SK, Dipole orientation effects on nonlinear optical properties of organic molecular aggregates. J Chem Phys 2003; 118: 8420–8427.
6. Benner AF, Ignatowski M, Kash JA, Kuchta DM, Ritter MB, Exploitation of optical interconnects in future server architectures. IBM J Res Dev 2005; 49: 755-775.
7. Lecaque LB, Coe BJ, Clays K, Foerier S, Verbiest T, Asselberghes I, J Am Chem Soc 2008; 130: 3286 -3287.
8. Sarma B, Nath NK, Bhogala BR, Nangia A, Synthon competition and cooperation in molecular salts of hydroxybenzoic acids and aminopyridines. Cryst Growth Des 2009; 9: 1546-1557.
9. Hemamalini M, Fun HK, 2-Amino-4-methylpyridinium 2 -hydroxybenzoate. Acta Crystallo graphica Section E 2010; E66: o2151–o2152.
10. Khalib NC, Thanigaimani K, Arshad S, AbdulRazak I, 2-Amino-4-methylpyridinium   3 –hydroxy benzoate. Acta Crystallographica Section E 2013; E69: o1120.
11. Sivakumar P, Sudhahar S, Israel CS, Chakkaravarthi G, 2-Amino-4-methylpyridinium   4-hydroxybenzoate. ICUR data 2016; 1-3.
12. Srinivasan TP, Anandhi S, Gopalakrishnan R, Growth and characterization of 2-amino-4-picolinium 4-aminobenzoate single crystals. Spectrochimica Acta Part A 2010; 75: 1223–1227.
13. Vasuki S, Karunakaran RT, Shanmugam G, Spectroscopic, quantum chemical, physical and antioxidant studies on 2-amino-4-picolinium 4-nitrobenzoate – an organic crystal for nonlinear optical and biological applications. Z Phys Chem 2016; 1-26.
14. Thirupugalmani K, Karthick S, Shanmugam G, Kannan V, Sridhar B, Nehru K et al. Second- and third-order nonlinear optical and quantum chemical studies on 2-amino-4-picolinium-nitrophenolate-nitrophenol: A phasematchable organic single crystal. Optical Materials 2015; 49: 158-170.
15. Bhogala BR, Nangia A, Ternary and quaternary co-crystals of 1,3-*cis*,5-*cis*-cyclohexane tricarboxylic acid and 4,4′-bipyridines. New J Chem 2008; 32: 800-807.
16. Santra R, Ghosh N, Biradha K, Crystal engineering with acid and pyridine heteromeric synthon: neutral and ionic co-crystals. New J Chem 2008; 32: 1673-1676.
17. Etter MC, Encoding and decoding hydrogen-bond patterns of organic compounds. Acc Chem Res 1990; 23: 120-126.
18. Etter MC, Hydrogen bonds as design elements in organic chemistry. J Phys Chem 1991; 95: 4601-4610.

19. Karthiga Devi P, Venkatachalam K, Poonkothai M, Spectroscopic, optical, thermal, antimicrobial and density functional theory studies of 4-aminopyridinium 4-hydroxy benzoate hydrate crystal. J Mol Struct 2016: xxx.
20. Al-Otaibi JS, Tautomerization, molecular structure, transition state structure, and vibrational spectra of 2-aminopyridines: a combined computational and experimental study. Springer Plus 2015; 586: 1 – 18.
21. Anandha Babu G, Ramasamy P, Growth and characterization of 2-amino-4-picolinium toluene sulfonate single crystal. Spectrochimica Acta Part A 2011; 82: 521 – 526.
22. Nakanishi W, Hitosugi S, Piskareva, H. Isobe, 1,8-Diiodo-anthracene. Acta Cryst 2010; o2515: E66.
23. Muthuraja P, Sethuram M, Shanmugavadivu T, Dhandapani M, Single crystal X-ray diffraction and Hirshfeld surface analyses of supramolecular assemblies in certain hydrogen bonded heterocyclic organic crystals. J Mol Struct 2016; 1122: 146–156.
24. Karabacak M, Kose E, Kurt M, FT-Raman, FT-IR spectra and DFT calculations on monomeric and dimeric structures of 5-fluoro- and 5-chloro-salicylic acid. J Raman Spectrosc 2010; 41: 1085–1097.
25. Amalanathan M, Hubert Joe I, Rastogi V.K, Density functional theory studies on molecular structure and vibrational spectra of NLO crystal L-phenylalanine phenylalanium nitrate for THz application. J Mol Stru 2011; 1006; 513–526.
26. Aditya Prasad A, Muthu K, Rajasekar M, Meenatchi V, Meenakshisundaram SP, Crystal growth, characterization and theoretical studies of 4-aminopyridinium picrate. Spectrochimica Acta Part A 2015; 135: 805 – 813.
27. Edwin B, Amalanathan M, Hubert Joe I, Vibrational spectra and natural bond orbital analysis of organic crystal L-prolinium picrate. Spectrochimica Acta Part A: Mol Biomol Spectro 2012; 96: 10–17.

Author(s) & affiliation

G. Dinesh kumar[a], G. Amirthaganesan[b]∗, P. Muthuraja[b], M. Dhandapani[b]

[a]Department of Chemistry, Gobi Arts & Science College, Gobichettipalayam, Tamilnadu, India.

[b]Department of Chemistry, Sri Ramakrishna Mission Vidyalaya College of Arts and Science, Coimbatore, Tamilnadu, India.

Corresponding Author: G. Amirthaganesan